BULLETIN OF THE EARTHQUAKE
RESEARCH INSTITUTE
Vol. 44 (1966), pp. 73-88

4. *Generation and Propagation of G Waves from the Niigata Earthquake of June 16, 1964. Part 2. Estimation of earthquake moment, released energy, and stress-strain drop from the G wave spectrum.*

By Keiiti AKI,

Earthquake Research Institute.

(Read July 20, 1965.—Received Dec. 17, 1965.)

Summary

Assuming a double couple (step function in time) as the source model and comparing the theoretical spectral density of G waves obtained by Haskell, Ben-Menahem and Harkrider with the observed, we estimated the magnitude of the moment of the component couple as 3×10^{27} dyne cm for the Niigata earthquake. By the dynamical equivalence of a double couple and a slip dislocation, average amount of dislocation $\bar{u}$ is obtained as $\bar{u}=\frac{M_0}{\mu S}$, where M_0 is the moment of the component couple of the equivalent double couple, μ is the rigidity and S is the area of fault surface. For a fault width 20 km and length 100 km, $\bar{u}$ is estimated as 400 cm, which agrees reasonably well with the average displacement discovered by an echo-sounding survey. The strain energy released by the formation of the fault is estimated by the use of Starr's formula as 5.0×10^{23} erg. The energy estimated from the magnitude ($M=7.5$) is 1.1×10^{23} erg. The magnitude of stress drop is estimated as 126 bars, and the corresponding strain drop 3.4×10^{-4}.

§ 1. Introduction.

There have been numerous investigations of the radiation pattern of P and S waves based on the assumption that an earthquake source is represented by a double couple or a single couple. In these studies, the geometrical aspects of the couple have been emphasized, but the magnitude of its moment, the only physical quantity relevant to a couple, has not attracted due attention, if not neglected. There is a reason for this, that is, the amplitudes of body waves with short wave lengths are influenced by fine structures of the crust-mantle, and it is difficult to eliminate their

effect to isolate source factors. Further, the amplitude at short periods is too sensitive to minor fluctuation of the source time function. These difficulties may not exist in long period surface waves. The effect of the structure complex may be eliminated in the mean amplitude spectral density obtained in Part 1.[1] We showed also that the source time function may be approximated by a step-function at least for period of 200 sec. Then, it is possible to find the height of the step in the step-function, that is, the magnitude of component couple of the assumed double couple, from the observed spectral density.

We shall proceed further to estimation of fault dislocation, released energy, and stress-strain drop on the basis of the dynamical equivalence between a double couple and a slip dislocation.

§ 2. Displacement spectral density.

In Part 1, we obtained the mean amplitude spectral density of $G2$ waves equalized to a lapse time of 7000 sec and to an epicentral distance of 90° in the loop directions (azimuth 0 to −30° and 150° to 180°) and in the node directions (0 to 45°), together with the Q values for each

Table 1. Observed mean displacement spectral density in radiation azimuths −30° to 0 and 150° to 180°

Freq. c/s	Period sec	Record amplitude			Magnification	Displacement	
		$\Delta=90°$ t=7000 sec cm sec	Correction* factor for Q	$\Delta=90°$ t=0 cm sec		$\Delta=90°$ t=0 cm sec	$\Delta=10{,}000$ km flattening** cm sec
.0050	200	79.5	3.34	266	70	3.80	3.03
.0065	154	101.3	4.70	476	140	3.40	2.71
.0080	125	113.2	5.37	671	210	3.20	2.55
.0095	105	127.4	9.03	948	275	3.45	2.75
.0110	91	123.0	8.76	1077	340	3.17	2.53
.0125	80	121.6	5.16	627	400	1.57	1.25
.0140	71	133.7	8.33	1114	450	2.48	1.98
.0155	65	110.3	10.4	1147	490	2.34	1.87
.0170	59	73.9	7.24	535	530	1.01	0.81
.0185	54	64.3	9.21	592	560	1.06	0.85
.0200	50	52.0	9.21	479	590	0.81	0.65

* $\exp(\pi \times 7000\,\text{sec}/QT)$, Q is taken from Table 15 of Part 1 and T is the period.
** multiplication of a factor of $\sqrt{R\,10000\,\text{km}}$, where R is the radius of the earth.

1) K. AKI, *Bull. Earthq. Res. Inst.*, 44 (1966), 23-72.

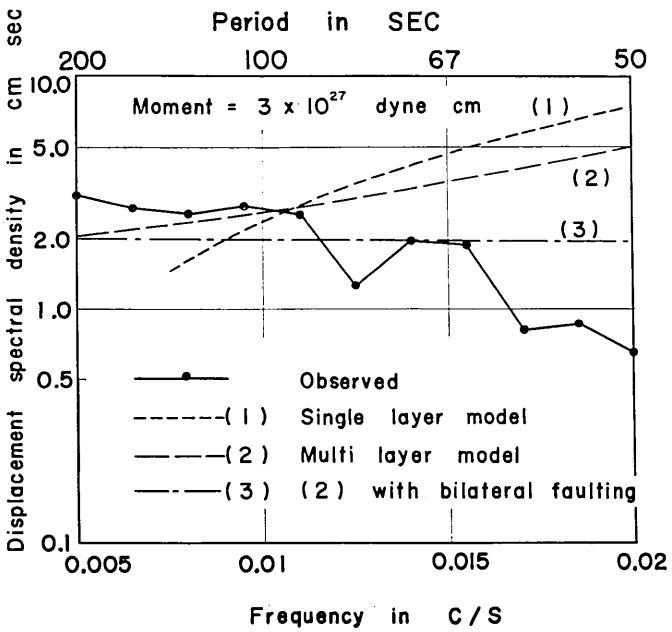

Fig. 1. Comparison of the observed displacement spectral density in the loop direction (equalized to a distance of 10,000 km on a non-dissipative flat earth model) with the theoretical predictions. The theoretical curve (1) corresponds to an earth model with a single layer crust overlying a uniform mantle. The curve (2) corresponds to a Gutenberg mantle model. The curve (3) is the curve (2) corrected for the effect of finiteness of the earthquake source. In all theoretical curves, the moment of the source couple is assumed as 3×10^{27} dyne cm.

direction. We shall first correct the spectral density for dissipation by multiplying a factor $\exp\{\pi\times 7000/QT\}$, where T is the period. The result is shown in Table 1 for the loop directions. Since the matter is more complicated for the node directions as described in Part 1, we shall only use the result for the loop direction for comparison with theoretical predictions.

The amplitude spectral density thus equalized to the origin time is then corrected for instrument magnification, which is also listed in Table 1. The result of this correction corresponds to the ground displacement at the epicentral distance of 90°, for a non-dissipative earth. For comparison with theoretical predictions based on flat earth models, a correction for flattening is applied as shown in Table 1. This result corresponds to the ground displacement at the epicentral distance of 10,000 km on a flat

non-dissipative earth. This value is plotted against frequency in Fig. 1.

§ 3. Comparison with theoretical predictions based on a single layer model.

According to Haskell,[2] for a model of single layer crust over a half space, the Love wave displacement $U_\varphi(t)$ at distance r from a buried double couple source with unit component moment varying in time as $e^{i\omega t}$ may be expressed as

$$\begin{aligned} U_\varphi(t)=2B(\lambda, r, h)[&-ir_{\beta 1}\tan(\lambda r_{\beta 1}h)\{(f_1n_3+f_3n_1)\sin\varphi \\ &-(f_2n_3+f_3n_2)\cos\varphi\} \\ &+(f_2n_2-f_1n_1)\sin 2\varphi \\ &+(f_1n_2+f_2n_1)\cos 2\varphi]e^{i\omega t}\ , \end{aligned} \tag{1}$$

where

$$\begin{aligned} B(\lambda, r, h)=&\{\rho_2\lambda\cos(\lambda r_{\beta 1}h)/4\rho_1\beta_1^2 r_{\beta 1}F'(\lambda)\sin(\lambda r_{\beta 1}d_1)\} \\ &\times(2/\pi\lambda r)^{1/2}\exp(-i\lambda r+i\pi/4)\ , \end{aligned} \tag{2}$$

$$F(k)=\rho_2\cosh\nu_{\beta 1}d_1+(\rho_1\beta_1^2\nu_{\beta 1}/\beta_2^2\nu_{\beta 2})\sinh\nu_{\beta 1}d_1\ , \tag{3}$$

$F(\lambda)=0$,
$r_{\beta 1}=\sqrt{(c/\beta_1)^2-1}$,
$r_{\beta 2}=\sqrt{1-(c/\beta_2)^2}$,
$\nu_{\beta 1}=i\sqrt{\omega^2/\beta_1^2-k^2}=ikr_{\beta 1}$,
$\nu_{\beta 2}=\sqrt{k^2-\omega^2/\beta_2^2}=kr_{\beta 2}$,

λ : wave number of Love waves,
c : phase velocity of Love waves,
h : depth of source,
β_1 : shear velocity in the crust,
ρ_1 : density in the crust,
β_2 : shear velocity in the mantle,
ρ_2 : density in the mantle,
d_1 : thickness of the crust,
f_1, f_2, f_3: direction cosines of force on the overhanging side,
n_1, n_2, n_3: direction cosines of normal of fault plane on the same side as above,
φ : station azimuth.

2) N. A. HASKELL, *Bull. Seis. Soc. Amer.*, 54 (1964), 377-394.

Based on the result obtained in Part 1 from the radiation pattern of the first motions and the $G2$ waves with period of 200 sec, we assume that the azimuth of dip-direction is N70°W, the dip of fault plane 70° and the fault motion is reverse dip-slip without strike-slip component. Then, taking the dip-direction as the x_2-axis, the x_3-axis downward, we get

$$\begin{aligned} f_1&=0, & n_1&=0\ , \\ f_2&=-\cos 70^\circ, & n_2&=\sin 70^\circ\ , \\ f_3&=-\sin 70^\circ, & n_3&=-\cos 70^\circ\ . \end{aligned}$$

The mean azimuth to stations in the loop direction is -35° from the fault strike. Using these values, Eq. 1 can be rewritten as

$$\begin{aligned} U_\varphi(0)&=2B(\lambda, r, h)\{-ir_{\beta 1}\tan(\lambda r_{\beta 1}h)(\sin^2 70^\circ-\cos^2 70^\circ)\cos 35^\circ \\ &\quad -\sin 70^\circ\cos 70^\circ\sin 70^\circ\} \\ &=-2B(\lambda, r, h)\{ir_{\beta 1}\tan(\lambda r_{\beta 1}h)\times(+0.627)+0.302\}\ . \end{aligned} \tag{4}$$

The absolute value of $U_\varphi(0)$ is then,

$$|U_\varphi(0)|=2|B(\lambda, r, h)|[(0.302)^2+\{0.627r_{\beta 1}\tan(\lambda r_{\beta 1}h)\}^2]^{1/2}\ . \tag{5}$$

In evaluating $|U_\varphi(0)|$ according to the above formula we assumed the parameters for the crust and mantle as follows,

$$\begin{aligned} \beta_1&=3.60\ \text{km/sec}\ , \\ \beta_2&=4.60\ \text{km/sec}\ , \\ \rho_1&=2.85\ \text{gr/cm}^3\ , \\ \rho_2&=3.28\ \text{gr/cm}^3\ , \\ d_1&=35\ \text{km}\ . \end{aligned}$$

Using the result of recomputation of the focal depth, we assumed the source depth h as one half of the crustal thickness d_1.

The process of computation is as follows. First, we compute the wave number for a given phase velocity c by the well-known formula,

$$\tan\lambda r_{\beta 1}d_1=\frac{\rho_2\beta_2^2 r_{\beta 2}}{\rho_1\beta_1^2 r_{\beta 1}}\ . \tag{6}$$

By a direct differentiation of $F(\lambda)$, we get

$$F'(\lambda)=\frac{\rho_2 d_1}{r_{\beta 1}}\sin(\lambda r_{\beta 1}d_1)+\frac{\rho_1\beta_1^2 d_1}{\beta_2^2 r_{\beta 2}}\cos(\lambda r_{\beta 1}d_1)$$
$$+\frac{\rho_1\beta_1^2 c^2}{\beta_2^2\lambda r_{\beta 2}^3 r_{\beta 1}}\left(\frac{1}{\beta_1^2}-\frac{1}{\beta_2^2}\right)\sin(\lambda r_{\beta 1}d_1)\,.$$

Using the relation $F(\lambda)=0$, we can rewrite this as

$$F'(\lambda)=\frac{\rho_1 c^2 d_1}{\beta_1^2 r_{\beta 2}r_{\beta 1}^2}\left\{\frac{\rho_2^2}{\rho_1^2}\left(\frac{\beta_2^2}{c^2}-1\right)+\frac{\beta_1^2}{\beta_2^2}\left(1-\frac{\beta_1^2}{c^2}\right)\right.$$
$$\left.+\frac{\rho_2}{\rho_1}\frac{1}{\lambda r_{\beta 2}d_1}\left(1-\frac{\beta_1^2}{\beta_2^2}\right)\right\}\cos(\lambda r_{\beta 1}d_1)\,. \qquad (7)$$

Inserting the above formula into Eq. (2), we get

$$B(\lambda, r, h)=\frac{\rho_2\lambda B_1 B_3}{2\rho_1 d_1 c^2 B_2}\,, \qquad (8)$$

where

$$B_1=\frac{r_{\beta 2}r_{\beta 1}\cos(\lambda r_{\beta 1}h)}{\sin(2\lambda r_{\beta 1}d_1)}\,,$$
$$B_2=\frac{\rho_2^2}{\rho_1^2}\left(\frac{\beta_2^2}{c^2}-1\right)+\frac{\beta_1^2}{\beta_2^2}\left(1-\frac{\beta_1^2}{c^2}\right)+\frac{\rho_2}{\rho_1}\left(1-\frac{\beta_1^2}{\beta_2^2}\right)\frac{1}{\lambda r_{\beta 2}d_1}\,,$$
$$B_3=(2/\pi\lambda r)^{1/2}\,.$$

The amplitude $|U_\varphi(0)|$ in Eq. (5) corresponds to the source of a sinusoidal time function. Since, as shown in Part 1, the absolute value of the observed source phase for period of 200 sec is consistent with the source of a step function in time, we shall compute the spectral density for such a source. If the moment of component couple of the source double couple varied as

$$M=0 \qquad t<0$$
$$=M_0 \text{ dyne cm} \qquad t>0\,,$$

the displacement spectral density will be $|U_\varphi(0)|\frac{M_0}{\omega}$, which can be written as

$$\frac{\rho_2}{2\rho_1 d_1 c^3}\cdot\frac{B_1 B_3}{B_2}\cdot M_0 G\,,$$

where

Table 2. Computation of displacement spectral density for a single layer model

C	km/sec	4.55	4.50	4.40	4.20	4.00
λd_1	radian	0.443	0.639	0.944	1.505	2.253
T	sec	109	76.5	53.0	34.8	24.5
$r_{\beta 1}$		0.773	0.750	0.702	0.602	0.484
$r_{\beta 2}$		0.147	0.207	0.291	0.408	0.494
B_1		0.1766	0.1848	0.1993	0.2274	0.2496
B_2		7.132	3.652	1.952	1.154	0.944
B_3		0.0710	0.0591	0.0486	0.0385	0.0315
$\frac{B_1 B_2}{B_3}$		0.001758	0.002990	0.004964	0.007583	0.00833
$\frac{\rho_2}{2\rho_1^2 d_1 C^3}$	10^{-24} dyne^{-1} sec	0.613	0.633	0.677	0.779	0.902
$\frac{B(\lambda, r, h)}{\omega}$	10^{-27} dyne^{-1} sec	1.08	1.89	3.36	5.91	7.51
G		0.628	0.648	0.674	0.708	0.708
$\frac{B(\lambda, r, h)}{\omega} G$	10^{-27} dyne^{-1} sec	0.68	1.22	2.26	4.18	5.32
$\frac{B(\lambda, r, h)}{\omega} G M_0$	cm sec	2.04	3.66	6.78	12.5	16.0

($M_0 = 3 \times 10^{27}$ dyne cm)

$$G = 2[(0.302)^2 + \{0.627 \cdot r_{\beta 1} \cdot \tan(\lambda r_{\beta 1} h)\}^2]^{1/2} .$$

Numerical computations are carried out for periods from 25 to 110 sec, as shown in Table 2. The displacement spectral density corresponding to the source with moment of 3×10^{27} dyne cm is given at the bottom of the table, and also shown in Fig. 1 (theoretical curve (1)).

Comparing this with the observed, we find that the theoretical value drops rapidly toward long periods, and increases with decreasing periods contrary to the observation. This is partly because we assumed an uniform mantle in the theoretical model, and partly because we neglected the finiteness of fault which tends to suppress short period waves.

§ 4. Multi-layer model.

Ben-Menahem and Harkrider[3] computed the displacement spectral density of Love and Rayleigh waves for various source models buried in a Gutenberg flat continental earth model. One of the cases, for which

3) A. BEN-MENAHEM and D. G. HARKRIDER, *J. Geophys. Res.*, **69** (1964), 2605–2620.

they gave numerical result, is nearly identical to the fault model we fitted to the Niigata earthquake. That is the one shown in their Fig. 23, where the fault motion is pure dip slip, and the dip angle of the fault plane is 15° (which is identical to 75° for a double couple). The maximum "reduced amplitude" is given as 447 $cm^{1/2}$/dyne for period of 55 sec for this source. Another case which is close to ours is the one shown in Fig. 22, where the dip angle is again 15° and there is a small strike-slip component. For this source, the maximum "reduced amplitude" is given as 71.3 $cm^{1/2}$/dyne for period of 167 sec.

The displacement spectral density corresponding to our observation may be computed by the use of their equation (58).

$$|U| = \frac{10^{-19}|R(\omega)|\,|n|}{(2\pi r)^{1/2}}|U^*| \text{ (micron sec)}$$

where $|R(\omega)|$ is the magnitude of the force in *CGS* unit, n is the unit normal vector to plane of motion measured in km,[4] r is the epicentral distance in km and $|U^*|$ is the "reduced amplitude" corrected for azimuthal effect. If we assume a step function source, $|R(\omega)| = \frac{R_0}{\omega}$, then we have

$$|U| = \frac{10^{-19}R_0|n|}{(2\pi r)^{1/2}}\frac{|U^*|}{\omega}\,. \tag{9}$$

Assuming the same amount of the moment of couple as in the single layer case, we have

$$R_0|n| = 3\times10^{27} \text{ dyne cm} = 3\times10^{22} \text{ dyne km}\,.$$

The epicentral distance r is 10,000 km. We find from Table 3 of the paper by Ben-Menahem and Harkrider, that U^* for period of 55 sec is 420 $cm^{1/2}$/dyne, and for period of 167 is 67.0 $cm^{1/2}$/dyne. Both values are corrected for the azimuth from the maximum direction.

For period of 55 sec, then,

$$\begin{aligned}|U| &= \frac{10^{-19}\times3\times10^{22}\times420\times55}{\sqrt{2\pi}\times10{,}000\times2\pi} \text{ (micron sec)}\\ &= 44.1\times10^3 \text{ micron sec}\\ &= 4.41 \text{ cm sec}\,.\end{aligned}$$

4) The unit of the normal vector n was not explicitly stated in the original paper 3). The result based on this formula does not reasonably compare with Haskell's result for Love waves in a single layer model, and with Lamb's for Rayleigh waves in a half space, unless the vector is measured in km. Upon the writer's inquiry, Dr. Ben-Menahem, in a personal communication, confirmed that this should be measured in km.

For period of 167 sec, we get

$$|U|=2.13 \text{ cm sec}.$$

These results are plotted in Fig. 1. A smooth curve (theoretical curve (2)) is drawn connecting the two points by taking into account the spectrum of transfer function given in Fig. 2 of their paper.

We see that the agreement with observation is much improved by adopting a more realistic earth model. However, there is still some discrepancy in the shorter periods, where the theoretical value is several times greater than the observed. This discrepancy may partly be due to an inadequate dissipation correction applied to the observed amplitude. As shown in Fig. 21 of Part 1, the Q value used for correction jumps to a high value at shorter periods than 90 sec. We cannot deny the possibility that these high Q values may not indicate the low loss for short periods, but result from an interference effect. If the true Q is smaller than that assumed, the observed spectral densities at shorter periods must become greater than those given in Fig. 1. It is, however, important to find how much finiteness effect would account for this apparent discrepancy.

§ 5. Bilateral faulting.

In Part 1 (Table 10 and 11), we found that no significant difference of amplitude exists between opposite azimuths, with exception only of $G3$ waves at period of 65 sec, where the amplitude radiated northward from the epicentre shows a slightly greater value. From this and from the relative position of the main shock epicentre to the aftershock area and the tsunami source area described in Part 1, we may conclude that the fault propagated in both ways for nearly equal length.

As shown by Ben-Menahem,[5] the transfer function for a unilateral fault with length L and rupture velocity v may be written as

$$\frac{1}{L}\int_0^L \exp\left\{i\omega\left(t-\frac{x}{v}-\frac{r-x\cos\theta}{c}\right)\right\}dx$$
$$=\frac{\sin X}{X}e^{-iX}\exp\left\{i\omega\left(t-\frac{r}{c}\right)\right\},$$

where $X=\frac{\omega L}{2}\left(\frac{1}{v}-\frac{\cos\theta}{c}\right)$, r and θ are, respectively, the distance and

5) A. BEN-MENAHEM, *Bull. Seis. Soc. Amer.*, **51** (1961), 401-435.

azimuth (measured from the direction of fault propagation) to a station, and c is the phase velocity of a wave.

For a symmetric bilateral faulting, the corresponding transfer function may be written as

$$\begin{aligned}&\frac{1}{L}\int_0^{L/2}\exp\left\{i\omega\left(t-\frac{x}{v}-\frac{r-x\cos\theta}{c}\right)\right\}dx\\&\quad+\frac{1}{L}\int_0^{L/2}\exp\left\{i\omega\left(t-\frac{x'}{v}-\frac{r+x'\cos\theta}{c}\right)\right\}dx'\\&=\frac{1}{2}\left(\frac{\sin X}{X}e^{-iX}+\frac{\sin Y}{Y}e^{-iY}\right)\exp\left\{i\omega\left(t-\frac{r}{c}\right)\right\}\end{aligned}\tag{10}$$

where

$$X=\frac{\omega L}{4}\left(\frac{1}{v}-\frac{\cos\theta}{c}\right)$$

$$Y=\frac{\omega L}{4}\left(\frac{1}{v}+\frac{\cos\theta}{c}\right).$$

The absolute value of this transfer function will be

$$\frac{1}{2}\left\{\frac{\sin^2 Y}{X^2}+\frac{\sin^2 Y}{Y^2}+2\frac{\sin X\sin Y}{XY}\cos(X-Y)\right\}^{1/2}.$$

For our case, the evidences from the aftershock area and the tsunami source area indicate a fault length L of about 100 km. Numerical evaluation of the above formula showed that for a significant suppression of the spectrum at the period range concerned, we must assign the rupture velocity less than about 1.5 km/sec. This is consistent with the value required to explain the observed source phase as discussed in § 10 of Part 1. Fig. 1 shows the result of such finiteness correction (curve (3)) applied to the theoretical curve for multilayer model (curve (2)), on the assumption that the total fault length is 100 km and the rupture velocity is 1.5 km/sec. The agreement with observation is generally improved by this correction. We cannot, however, conclude definitely that the rupture velocity must be smaller than 1.5 km/sec, because, as mentioned in the preceding section, there is an uncertainty in the dissipation correction applied to the observed at shorter periods.

On the other hand, the magnitude of the moment of source couple seems to be well determined from the observation at periods 100 to 200 sec. A value of 3×10^{27} dyne cm is probably the lowest estimate, and the

value seems not to exceed 4×10^{27} dyne cm. This precision of measurement is certainly much better than that of measurement of earthquake energy. We shall now discuss what this moment value means.

§ 6. Estimation of fault dislocation from the moment of source couple.

According to recent theoretical studies,[6),7),8)] the equivalency of a slip dislocation along a fault to a double couple in the absense of the fault is shown to be valid not only in the static elastic field but also in the dynamic elastic field.

Following Burridge and Knopoff,[9)] we take a rectangular cartesian coordinate system (x_1, x_2, x_3), and assume that a tangential displacement of the material in $x_3>0$ occurs relative to that in $x_3<0$. The discontinuities in displacement is specified in time and space as

$$[U_1]=\delta(x_1)\delta(x_2)H(t)\ ,$$
$$[U_2]=0\ ,$$
$$[U_3]=0\ ,$$

where $\delta(x_1)$ is the Dirac δ-function, $H(t)$ is the Heaviside unit-step function. According to Burridge and Knopoff, the equivalent body forces to the above dislocation is expressed as

$$e_1(x_1, x_2, x_3, t)=-\mu\delta(x_1)\dot{\delta}(x_2)\delta(x_3)H(t)$$
$$e_2(x_1, x_2, x_3, t)=0$$
$$e_3(x_1, x_2, x_3, t)=-\mu\dot{\delta}(x_1)\delta(x_2)\delta(x_3)H(t)\ ,$$

where μ is the rigidity. This is the double couple which begins to act at $t=0$ and is held at a constant level for $t>0$. We may obtain the moment M_0 of the component couple from the above expression as follows.

$$\begin{aligned} M_0&=\iiint e_1(x_1, x_2, x_3, t)x_3dx_1dx_2dx_3 \\ &=-\mu\int[U_1]dx_1dx_2\int x_3\dot{\delta}(x_3)dx_3 \\ &=\mu\int[U_1]dx_1dx_2\ . \end{aligned} \tag{11}$$

6) L. KNOPOFF and F. GILBERT, *Bull. Seis. Soc. Amer.*, **50** (1960), 117-134.
7) T. MARUYAMA, *Bull. Earthq. Res. Inst.*, **41** (1963), 467-486.
8) N. A. HASKELL, *Bull. Seis. Soc. Amer.*, **54** (1964), 1811-1841.
9) R. BURRIDGE and L. KNOPOFF, *Bull. Seis. Soc. Amer.*, **54** (1964), 1875-1888.

The last integral in the above equation may be regarded as the product of the area S of the fault surface and the average dislocation $\bar{u}$ over it. Then, we have

$$M_0 = \mu \bar{u} S \tag{12}$$

which relates the moment obtained from seismic waves to the area of fault surface and the amount of dislocation.[10]

In the case of the Niigata earthquake, we may take the fault length of 100 km (length of after-shock area) and its width of 20 km (an estimate of the focal depth of the main shock). The rigidity μ may be computed from the shear velocity (3.6 km/sec) and the density (2.85 gr/cm^3) in the crust. Then, we get from Eq. 12,

$$\bar{u} = \frac{3 \times 10^{27}(\text{dyne cm})}{3.7 \times 10^{11}(\text{dyne cm}^{-2}) 20 \times 100 \times 10^{10}(\text{cm}^2)}$$
$$= 400 \text{ cm} .$$

The average dislocation of 400 cm thus obtained reasonably agrees with the amount of upheavals (the maximum exceeding 5 meters) and subsidences (the maximum 4 meters) revealled by the echo-sounding survey[11] carried out in the epicentral ares before and after the earthquake.

§ 7. Estimation of released energy and stress-strain drop.

Let us estimate how much strain energy may be released by a formation of such a fault as described in the preceding section. We shall consider an infinite strip of crack, where a slip occurs along the crack perpendicular to the direction of strip. This will roughly represent a dip slip earthquake. Starr[12] obtained the elastic energy W released by the formation of such a crack in an infinite body which is clamped at infinity and was in a state of uniform shear stress σ before the crack was formed. He found that the energy per strip length L is

$$W = \frac{\pi}{4} \sigma^2 c^2 \frac{\lambda + 2\mu}{\mu(\lambda + \mu)} L , \tag{13}$$

10) Recently, this relation was independently discussed by TENG and BEN-MENAHEM (*J. Geophys. Res.*, **70** (1965), p. 5169). Their corresponding equation (Eq. 23), however, does not agree with ours and contradicts the theoretical results of MARUYAMA (*loc. cit.*, 7), BURRIDGE and KNOPOFF (*loc. cit.*, 9), and HASKELL (*loc. cit.*, 8).

11) A. MOGI, B. KAWAMURA and Y. IWABUCHI, *Jour. Geod. Soc. Japan*, **10** (1964), 180-186.

12) A. T. STARR, *Cambridge Philos. Soc. Proc.*, **24** (1928), 489-500.

where $2c$ is the width of strip-shaped fault, L is the length of the strip, and λ, μ are Lame's constants. On the other hand, the maximum relative displacement u_m along the crack is expressed as

$$u_m=\sigma c(\lambda+2\mu)\mu^{-1}(\lambda+\mu)^{-1}\,. \tag{14}$$

The average relative displacement $\bar{u}$ is $\frac{\pi}{4}u_m$. Assuming $\lambda=\mu$, we get from Eq. 13 and 14,

$$W=\frac{8}{3\pi}\bar{u}^2\mu L \tag{15}$$

Using the numerical values obtained in the preceding section we get

$$\begin{aligned}W&=0.85\times 3.7\times 10^{11}\times(400)^2\times 100\times 10^5\\&=5.0\times 10^{23}\ \text{erg}\,.\end{aligned}$$

This value is reasonably greater than the seismic energy estimated from the magnitude of the earthquake ($M=7.5$). The Gutenberg-Richter's formula, $\log E=11.8+1.5M$, gives the seismic energy for $M=7.5$,

$$E=1.1\times 10^{23}\ \text{erg}\,.$$

We may further estimate the pre-existed stress σ by Eq. 14, which can be rewritten for $\lambda=\mu$ as

$$\sigma=\frac{2}{3}\mu\frac{u_m}{c}=\frac{8}{3\pi}\mu\frac{\bar{u}}{c}\,. \tag{16}$$

If the fault width $2c$ is 20 km, we obtain

$$\sigma=0.85\times 3.7\times 10^{11}\times\frac{400}{10^6}=126\ \text{bars}\,.$$

The corresponding shear strain will be

$$\varepsilon=3.4\times 10^{-4}\,.$$

This value of strain agrees well with the tilting of about 1 minute (3×10^{-4} radian) observed by Nakamura etal.[13] at Awashima located at several kilometers from the epicentre. It also agrees with the ultimate

13) K. NAKAMURA, K. KASAHARA and T. MATSUDA, *Jour. Geod. Soc. Japan*, **10** (1964), 172-179,

strain of the earth's crust estimated from the geodetic observation on the crustal movements accompanied by other destructive earthquakes. For example, Tsuboi[14] estimates the ultimate strain as 1 to 2×10^{-4}, and Byerly-DeNoyer's[15] curve indicates the maximum strain of 6.3×10^{-4} for the 1906 San Andreas earthquake.

Reasonable values of dislocation, released energy and stress-strain drop well harmonized with the field observations strongly support the assumptions we made in estimating these values, including the basic one that an earthquake is a release of accumulated elastic strain by a rupture.

It must be emphasized here that although there are many assumptions involved, our estimation is based on the measurement of seismic waves, and therefore the ultimate strain obtained from this source is directly related to the interior of the crust, while the estimation by geodetic methods is concerned with the earth's surface.

It is interesting to note that the strength of the interior of the crust as estimated above seems to be too low to sustain the grest mountains and ocean trenches. Jeffreys'[16] conclusion on this problem is that the stress-differences of at least 1500 bars exist within the outermost 50 km of the earth. The stress-difference (the algebraic difference between the maximum and minimum principal stresses) for the case of the Niigata earthquake is estimated as about 250 bars (twice the maximum shear). This shows that the strength of the crust measured by an earthquake apparently cannot sustain the mountains and trenches.

§ 8. Some implications of the earthquake moment.

If we rewrite Starr's formula for released energy in terms of the pre-existed stress σ, the average dislocation $\bar{u}$ and the area S of the fault surface, we get from Eqs. (13) and (14),

$$W=\frac{1}{2}\sigma\bar{u}S\,. \tag{17}$$

Comparing the above equation with Eq. (12), we find that the product of the average dislocation $\bar{u}$ and the fault area S is common in both equations. The ratio of energy to moment becomes independent of $\bar{u}$ and S, and is equal to half the ratio of stress σ to rigidity μ.

14) C. TSUBOI, *Erg. d. kos. Physik*, 4 (1939), 106-168.

15) P. BYERLY and J. DENOYER, *Contributions in Geophysics in Honor of Beno Gutenberg* (Pergamon Press, New York and London 1958), pp. 17-35.

16) H. JEFFREYS, *The Earth, 4th ed.* (Cambridge Univ. Press, 1959), pp. 195-210.

$$\frac{W}{M_0} = \frac{\sigma}{2\mu} \,. \tag{18}$$

The above equation tells us that, if the earthquake source is a Starr fracture, the pre-existed stress σ may be estimated from the released energy and the earthquake moment, without the knowledge of the area of the fault surface and the amount of dislocation. The released energy may be found from the energy radiated in seismic waves if we know the efficiency of seismic radiation. Then, we may determine the stress drop entirely from the record of seismic waves. Although we don't know well about the efficiency of radiation at present, this method may become useful in the study of deep earthquakes and small shallow earthquakes for which we have no way of measuring the size of fault other than the seismometric method.

It is interesting to note that the above ratio roughly corresponds to one of the most effective diagnostic parameters used for distinguishing nuclear explosions from earthquakes. The parameter is the energy carried by long-period surface waves relative to the total seismic energy; it was found[17),18)] that for a given magnitude (for a given total seismic energy), earthquakes show a greater amount of long-period waves than explosions. Since the earthquake moment, as described in preceding sections, is proportional to the displacement spectral density at long periods where the assumption of step function holds, the greater amount of long-period waves will mean the greater moment, and for fixed total energy it will mean a smaller stress drop. Thus, the above findings imply a smaller stress drop in earthquakes than in explosions, as should be expected. Of course, we cannot apply the dislocation model to an explosion, and we need more refined theory and experiment to substantiate this conjecture. However, this seems to indicate the importance of the ratio of earthquake energy to moment as a measure of stress drop.

Acknowledgement.

The author gratefully acknowledges valuable discussions with Dr. T. Maruyama of the Earthquake Research Institute on the theoretical aspects of the present paper.

17) J. BRUNE, A. ESPINOSA and J. OLIVER, *J. Geophys. Res.*, **68** (1963), 3501-3514.
18) F. PRESS, G. DEWART and R. GILMAN, *J. Geophys. Res.*, **68** (1963), 2909-2928.

4. 1964年6月16日新潟地震によるG波の発生と伝播

(2) G波スペクトルより推定した地震モーメント，歪みエネルギーおよび初期歪みと応力

地震研究所　安芸敬一

時間的に階段函数であるような double couple の震源を仮定し，理論的に求めたスペクトルと実測値とを比較した．その結果，新潟地震のモーメントとして 3×10^{27} ダイン糎という値が得られた．辻り断層と double couple の等価関係から，このモーメントは，断層面積と変位と剛性率の積になる．断層の長さを100粁，幅を20粁と仮定して，得られたモーメントから断層変位を求めると4米となつた．これは音響測深の結果と大体一致する．このような断層によつて解放された歪みエネルギーの値は 5.0×10^{23} エルグとなり，マグニチュード(7.5)から求められる地震波のエネルギー 1.1×10^{23} エルグと矛盾しない．更に，このような断層を生じた初期応力は126気圧，対応する歪みは 3.4×10^{-4} となり，これらの値も地表で観測された地殻変動の結果と大体一致する．

このように，地震波から推定された震源の性質が，地表で調査された結果とよく調和することは，推定に用いた仮設の妥当であつたことを示す．すなわち，われわれの結果は，地震とは，地殻内部に貯えられた歪みエネルギーが断層の生成によつて放出する現象であるという仮設を支持するものである．